Supplemental Information

Engineering a microbial platform for *de novo* biosynthesis of diverse methylxanthines

Maureen McKeague[‡1], Yen-Hsiang Wang[‡1], Aaron Cravens[1], Maung Nyan Win[2], Christina D. Smolke[1]

1. Department of Bioengineering; 443 Via Ortega, MC 4245; Stanford University; Stanford, CA 94305

2. Synthetic Genomics; La Jolla, CA 92037

‡*These authors contributed equally to this work*

Contents

Supplemental Methods

Separation of paraxanthine and theophylline

Samples were analyzed by LC–MS/MS using an Agilent 1260 infinity binary pump HPLC and Agilent 6420 triple quadrupole mass spectrometer with an electrospray ionization source. To separate paraxanthine from theophylline, chromatography was performed as described by Choi and coworkers with some modifications (Choi et al., 2013). An Agilent Poroshell 120 EC-C_{18} column (3.0 × 50 mm, 2.7 μm) was used. Mobile phase A was water with 0.2% formic acid, phase B was methanol. The flow rate was 0.5 mL/min at 35 °C. 2 μL samples were injected and separated using an isocratic method of 15% B for 7 min. The eluent was directed to the MS for 0.8-5 min with ESI source gas temperature at 350 °C, gas flow of 11 L/min, nebulizer pressure of 40 PSI. The quantification of small molecules was based on the integrated peak area of the MRM chromatograms. The MRM transitions used are listed in Table 3, each of which was determined using the MassHunter Optimizer software with appropriate standards. MRM peak areas were compared to a calibration curve of external standard peak areas to determine concentration.

Measurement of intracellular metabolites

Yeast cultures were grown in 5 mL culture media in glass tubes. Single colonies of each strain were inoculated in triplicate into YNB media under appropriate dropout selection conditions, and grown overnight at 30 °C. The next day, the stationary phase culture was back-diluted and grown for an additional 3 or 6 days before harvesting the media for metabolite characterization. Samples were centrifuged at 15,000 rpm (10 min, 4 °C) to pellet the cells. Total volume of the cells was carefully measured. The supernatant was carefully sampled without disturbing the cell pellet. The remaining supernatant was completely removed and discarded. Intracellular metabolites were extracted by adding 500 μL acetone with vigorous shaking for 5 min. An addition 500 μL of water was added to ensure solubility of all methylxanthines. Samples were centrifuged at 15,000 rpm (10 min, 4 °C) to pellet the cell debris. The acetone-water mixture was carefully removed and concentrated to 1/10 of the original recorded cell volume. Both the supernatant and the concentration extracted intracellular contents were analyzed by LC–MS/MS using an Agilent 1260 infinity binary pump HPLC and Agilent 6420 triple quadrupole mass spectrometer with an electrospray ionization source as described in Section 2.4.

Analysis of cellular growth and methylxanthine toxicity

Yeast cells were grown in 300 μL of YNB under proper selection conditions in 2 mL deep well 96-well plates (as described in the section 2.3) with or without fed methylxanthines. The cell count and viability were measured using flow cytometry (MACSQuant VYB flow cytometer, Miltenyi Biotec Inc.). 10 μL of yeast culture media were sampled at given time point, and the samples were spun down at 4,500 rpm (5 min, 4 °C). The culture supernatant was discarded, and the cells were re-suspended in 200 μL of 1x phosphate buffered saline (PBS) with 1% bovine serum albumin (BSA Fraction V, EMD Millipore) and 1 mg/L DAPI (Life Technologies) as

viable cell stain. The cells were filtered with a nylon 6/6 woven mesh sheet (30 μm in mesh size and 40 μm in thread diameter; part # B000FMYHXO from Amazon) to remove large cell debris. DAPI was excited at 405 nm and captured by a 450/50 bandpass filter (channel V1 with PMT voltage 303).
The raw data were first converted into FlowJo-compatible format (FCS3.1), and data processing was performed using the standard software package FlowJo (Mac ver. X). The total viable cell counts were obtained through two consecutive gates: 1) scatter gate: side scatter (log) vs. forward scatter (linear); 2) viability gate: side scatter (log) vs. negative DAPI region (log). Cell viability was obtained by calculating the percentage of cells in the viability gate to those in the scatter gate.

Overexpression of *SAM2*

An extra copy of the endogenous yeast *SAM2* was overexpressed on a low-copy expression plasmid (HIS selection) and transformed into our methylxanthine producing strains for production of S-adenosyl-L-methionine (SAM) (Brown et al., 2015; Chu et al., 2013). An empty HIS vector was separately transformed into identical strains as a control. Each base strain, as well as the strain transformed with *SAM2* or the empty vector was grown in the absence or presence of 600 mg/L L-methionine (Schlenk and Depalma, 1957).After 6-days of culture, the production of the major end-product was measured as described by LC-MS (section 2.4).

Rough estimation of titers needed for approaching commercialization of microbial methylxanthine production
To obtain the cost of producing methylxanthines and their derivatives at industrial scales can be challenging, as most of the information about methylxanthine production (either through chemical synthesis or plant extraction) are proprietary knowledge. Rough estimates of the cost of producing methylxanthines were based on the market price at which methylxanthines are sold in bulk (i.e., kilogram level). Prices were obtained from a specialty chemical supplier (Made-In-China, http://www.made-in-china.com). The range of prices of specific methylxanthines are listed as following: active pharmaceutical grade (API) theophylline ($30-37 per kg), caffeine ($3-200 per kg), theobromine ($12-100 per kg), and aminophylline/doxofylline/diprophylline ($17-70 per kg). Assuming a base cost for the microbial fermentation and purification process (~$2/L), the break-even point is in the range of tens of grams per liter to one hundred grams per liter for current methylxanthines sold on the market.

Supplemental Results

Assessing toxicity of end-products

One of the reasons we chose to construct the methylxanthine pathway in yeast stemmed from previous work demonstrating the toxicity of caffeine to bacterial hosts such as *E. coli* (Sandlie et al., 1980), whereas this compound exhibits lower toxicity to yeast (Kuranda et al., 2006). Nevertheless, we sought to investigate the impact of high concentrations of the methylxanthine end-products on the growth and viability of our background yeast strain CSY893. Time course

cellular growth assays with CSY893 were performed using the four main methylxanthine end-products (1-methylxanthine, 3-methylxanthine, theophylline, and caffeine). Growth was assayed at mid-level concentrations, (16.7 -19.4 mg/L), high-level concentrations (83.5 -97.0 mg/L), and no fed methylxanthines. These concentrations represent titers that are up to 150-fold higher than that currently achieved with the engineered strains. The viable cell counts and percentage viability were measured over the course of experiment for a 6 day period. The results (Fig. S7) demonstrate that there is no significant impact on growth or viability of the strains, highlighting that yeast is an appropriate host for methylxanthine biosynthesis.

Optimizing strain performance through overexpression of *SAM2*

Previous results in *E. coli* have shown that SAM-dependent methylation can be a limited by SAM availability. For example, the *de novo* production of vanillin increased more than 25% through engineering SAM regeneration by overexpression of native genes and deregulation of SAM biosynthesis (Kunjapur et al., 2016). A similar strategy was recently pursued to facilitate *de novo* production of the alkaloid strictosidine in yeast (Brown et al., 2015). To investigate whether overexpression of *SAM2* would be beneficial for our engineering strains, we transformed our strains with an extra copy of the endogenous yeast *SAM2* and compared the end-product titers with the appropriate empty-vector control. Furthermore, since methionine is required for production of SAM, we also compared the effect of adding an additional 600 mg/L of L-methionine (Schlenk and Depalma, 1957) (a 30 fold excess to the 20 mg/L present in our standard growth media). After 6 days of culture, we observed no difference in production of our end-products (7-methylxanthine and caffeine) in the presence of excess L-methionine or with *SAM2* overexpression, or in combination of both excess L-methionine and *SAM2* overexpression. Our results (Fig. S8) suggest that SAM is not limiting to diverting flux into the *de novo* pathway (Fig. 1) nor is it required for enhanced methyltransferase activity in our current strains.

Comparing intracellular and extracellular methylxanthine concentrations

As a starting point for improving strain production titers, we examined whether certain pathway intermediates were accumulating in the media, and could thereby highlight pathway bottlenecks to production of the end-products. Titers of intermediates and end-products in the cell pellets (intracellular) and in the medium (extracellular) were measured after 3, 6, and 9 days, for the three engineered strains CSY1133, 1136, and 1139. Our results show that no particular methylxanthine is at significantly different concentrations from each other intracellularly. However, all methylxanthine metabolites were approximately one order of magnitude lower in concentration intracellularly compared to their measured extracellular concentrations (Fig. S9). This is consistent with purine alkaloid work performed in a closely related fungi, *Ashbya gossypii* (Ledesma-Amaro et al., 2015) and suggests efficient transport of these metabolites from the cell into the media. Given the high K_m of the methyltransferases used in the engineered strains, this may account for relatively low titer of the end-products. However, for the caffeine-producing strain (CSY1133) there is an accumulation of 7-methylxanthine in the media (Fig. S9) compared to theobromine; therefore indicating a potential point for future optimization. .

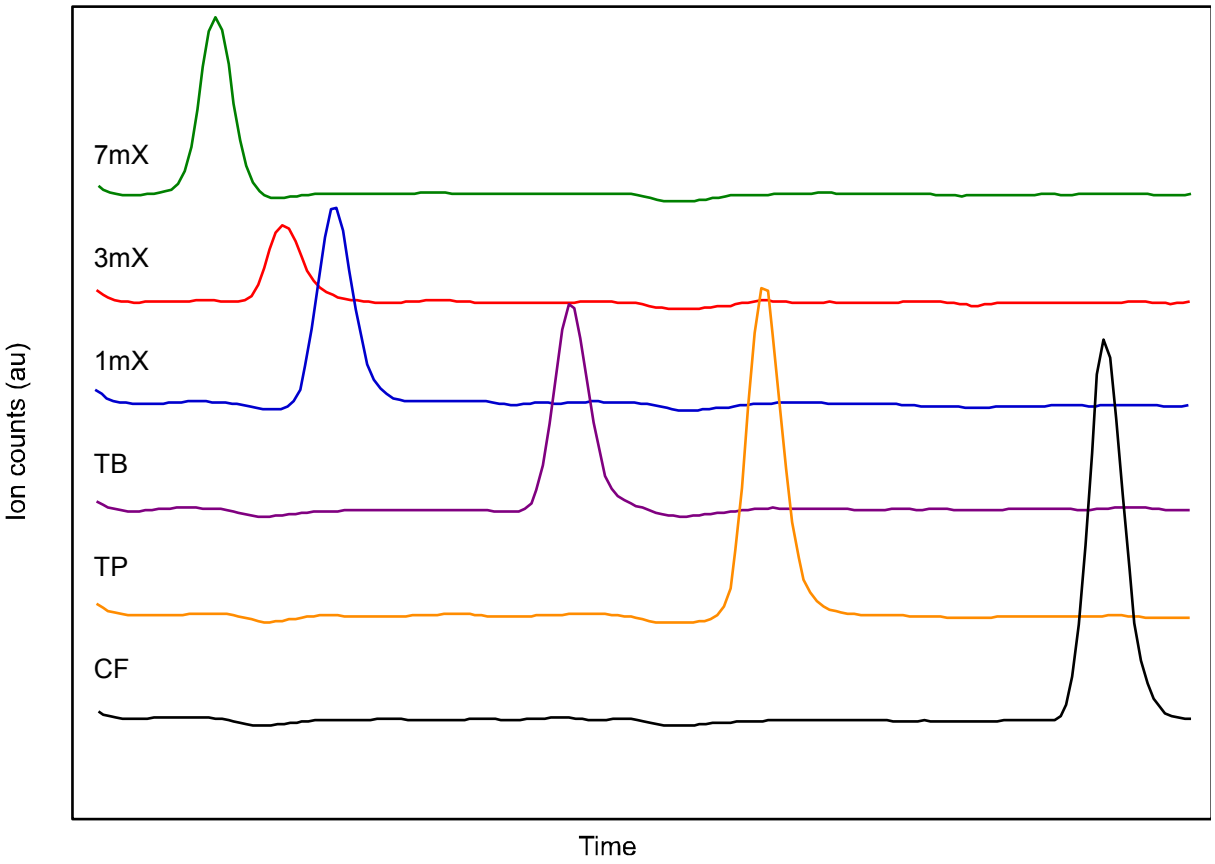

Fig. S1. LC-MS chromatograms (total ion count) of commercially-available methylxanthine standards to determine their production in yeast.

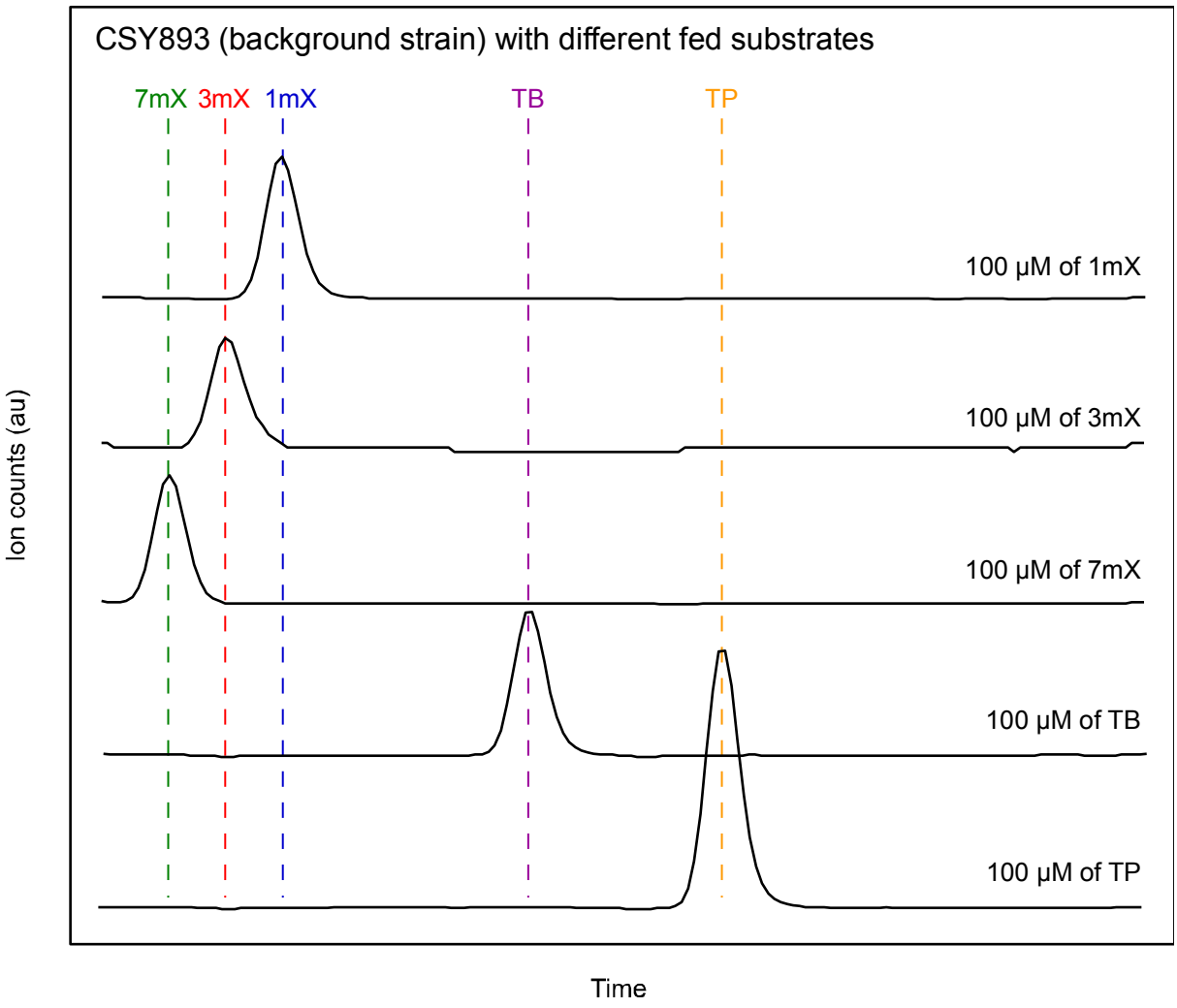

Fig. S2. LC-MS chromatograms (total ion count) of background strain CSY893 when feeding 100 µM of each methylxanthine substrate. No methylxanthine production was detected in the culture media.

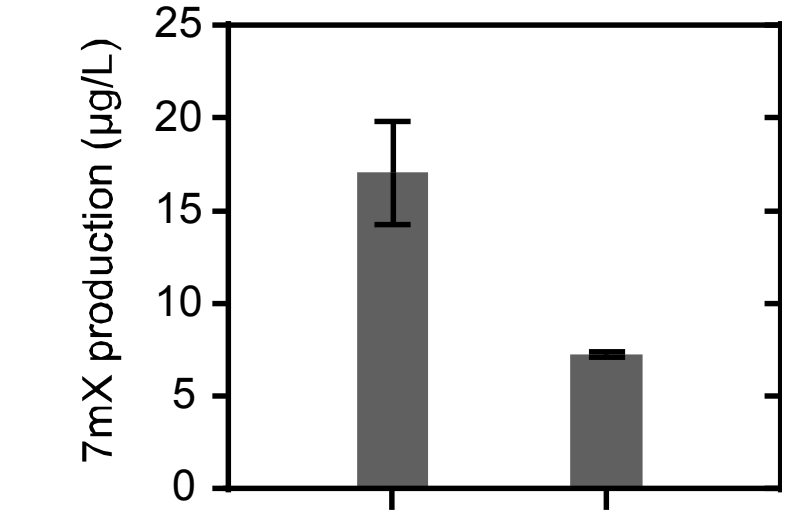

Strain (CSY#)	1125	1126
PA0065	int	int
XPT1	int	int
XMT1	int (CaXMT1)	int(yXMT1)

Fig. S3. Effect of yeast-codon optimization of XMT1 on 7-methylxanthine production. The plot shows the production of 7-methylxanthine of two strains (either with original or yeast-codon optimized XMT1) after 3 days of culture (YNB-DO with 2% dextrose). Production of 7-methylxanthine was analyzed by LC–MS/MS and data were reported as the mean and standard deviation of biological triplicates. Relevant genetic contents for each strain are displayed below the horizontal bar under each plot (see Table 1 for complete strain information).

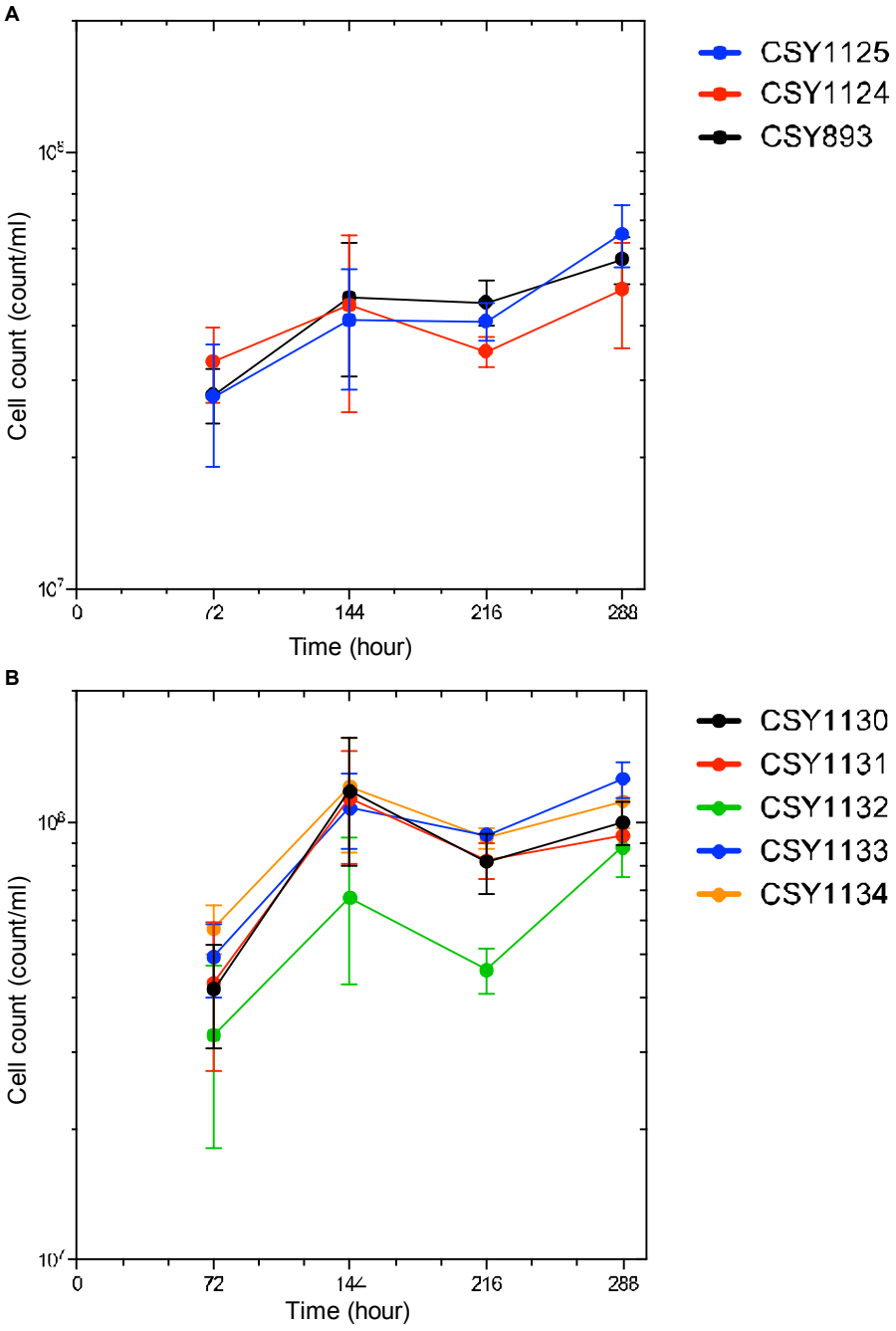

Fig. S4. Comparison of cell growth of engineered strains. Time course cellular growth assays with engineered strains. Strains were grown as described (section 2.3). Viable cell counts were measured over the course of the experiment. (A) Cell growth profiles for strains engineered for the production of 7-methylxanthine (Fig. 2) compared to the background strain CSY893. (B) Cell growth profiles of strains optimized for caffeine production (Fig. 3). Data are plotted as the mean values and error bars represent ± 1 s.d. of three biological replicates.

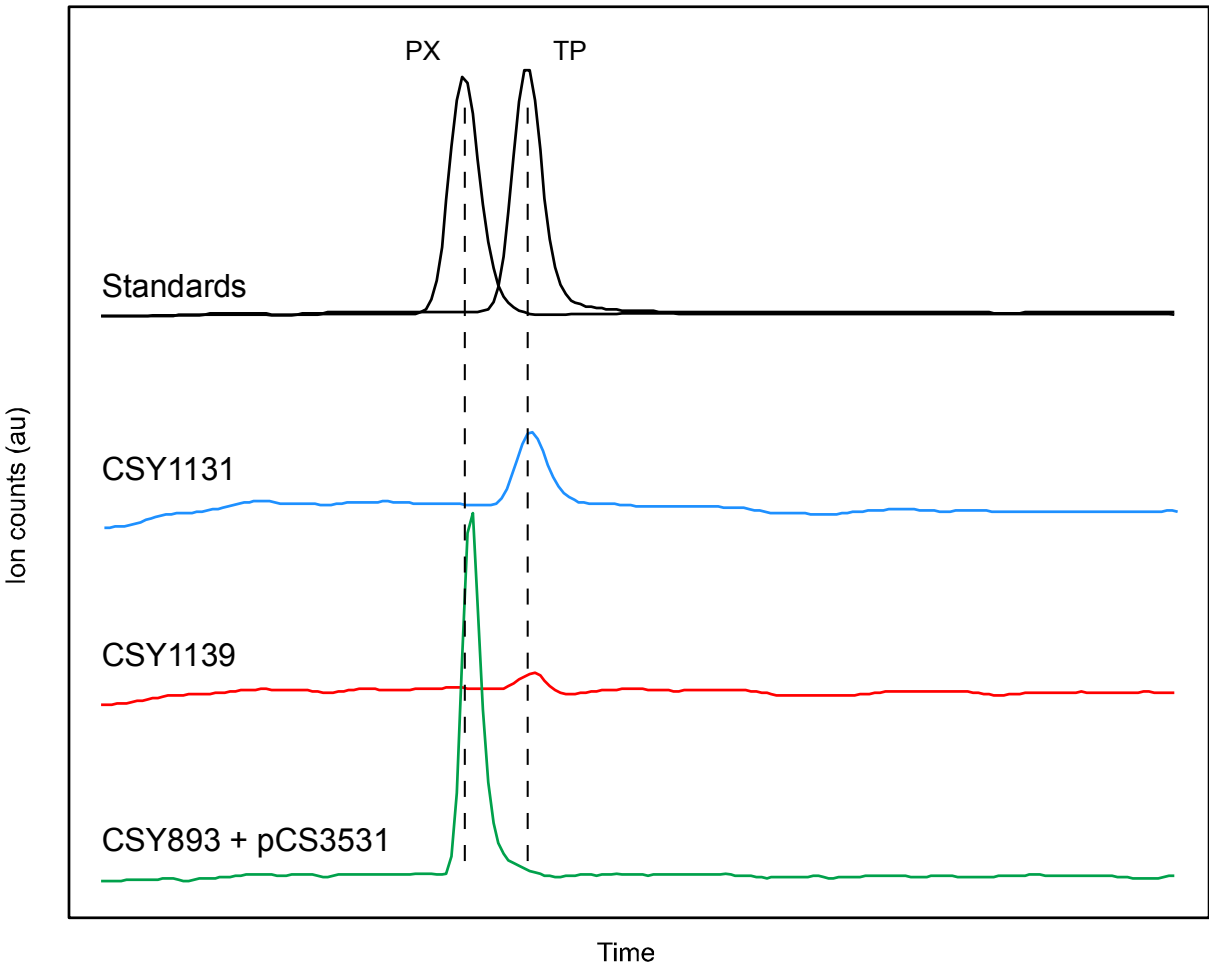

Fig. S5. Further separation of two co-eluted dimethylxanthines to confirm theophylline production in strains CSY1131 and 1139. Paraxanthine is only produced in background strain CSY893 expressing yCCS1 (pCS3531) with feeding 100 µM of 7-methylxanthine (see Table 4). See Supplementary Methods for details of the chromatography method to separate the two co-eluted dimethylxanthines (paraxanthine and theophylline).

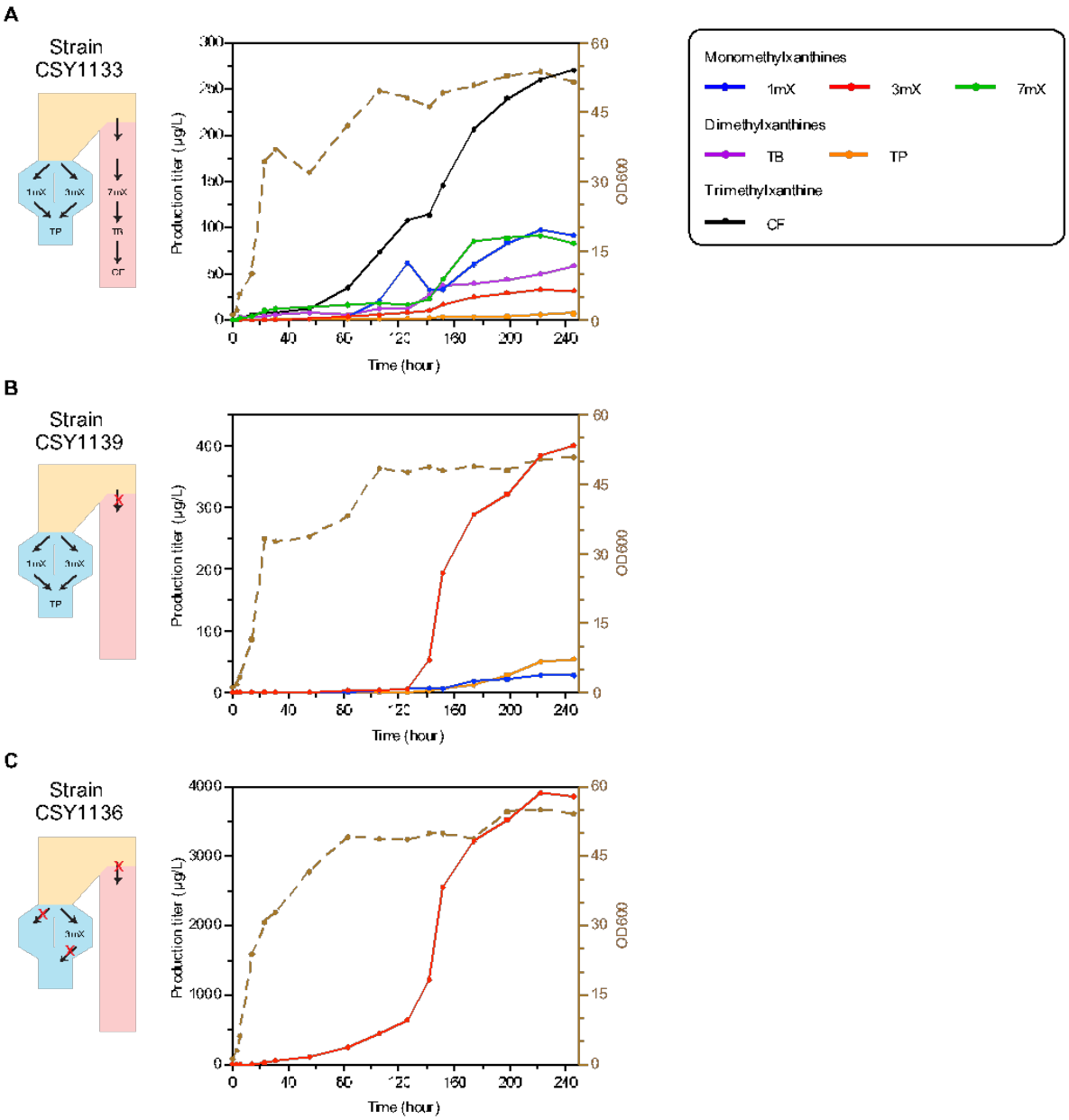

Fig. S6. 10-day bench scale batch fermentation for the production of diverse methylxanthines. Cell density and concentrations of indicated metabolites are shown as a function of time for the fermentation of *S. cerevisiae* strains: (A) CSY1133, (B) CSY1139, and (C) CSY1136. Corresponding engineered pathways for each strain are displayed on the left hand side of each panel. At indicated time points, samples were taken, diluted, and analyzed for cell density (OD600, brown y-axis on the right) through spectrometry and methylxanthine production through LC-MS/MS (black y-axis on the left). The analysis was performed on media supernatant collected at 152 hour of culture. LC traces shown are the quantifier +ESI MRM of each compound (see details in Table 3). Note, for this 10-day experiment, CSY1133 (noted to improve the production ratio of CF:THEO in Fig. 3C) was used in place of CSY1131.

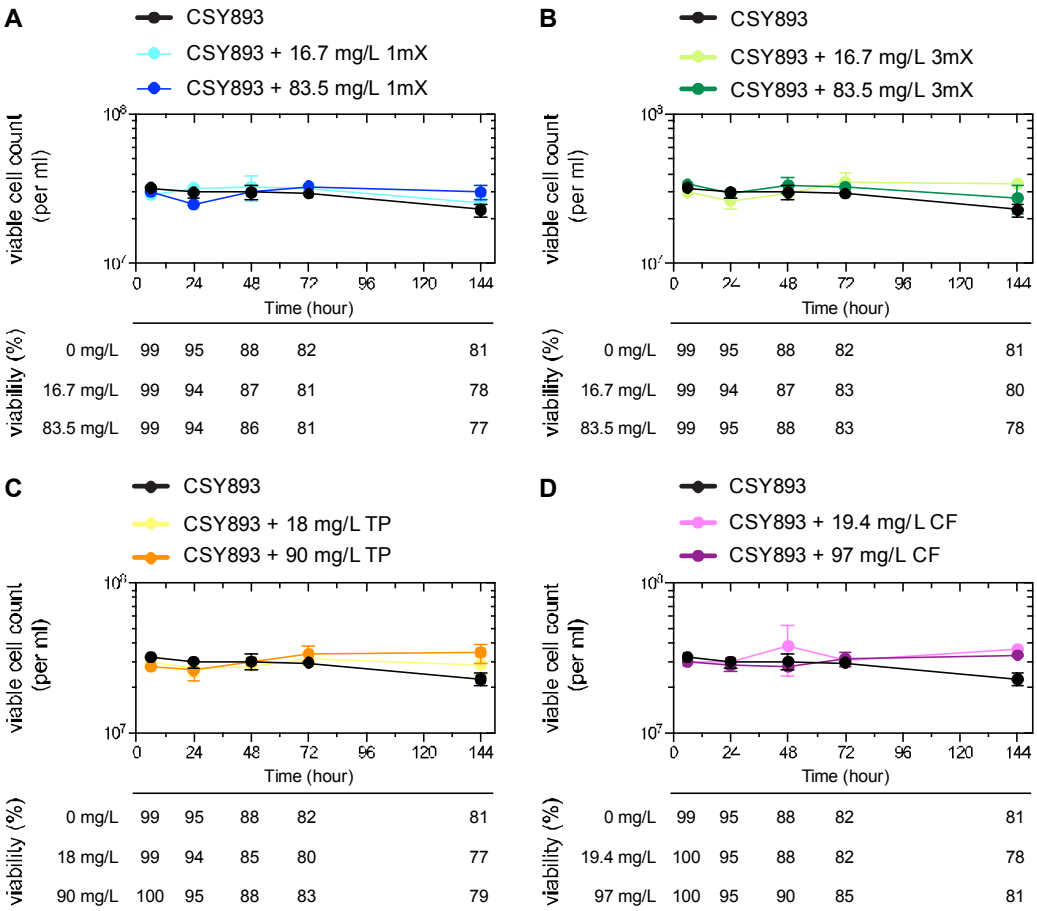

Fig. S7. Effect of methylxanthine end-products on cell viability. Time course cellular growth assays with CSY893 were performed using four methylxanthine products (1-methylxanthine, 3-methylxanthine, theophylline, and caffeine; concentration in mg/L indicated at the top of each plot). Viable cell counts and percentage viability were measured over the course of experiment.

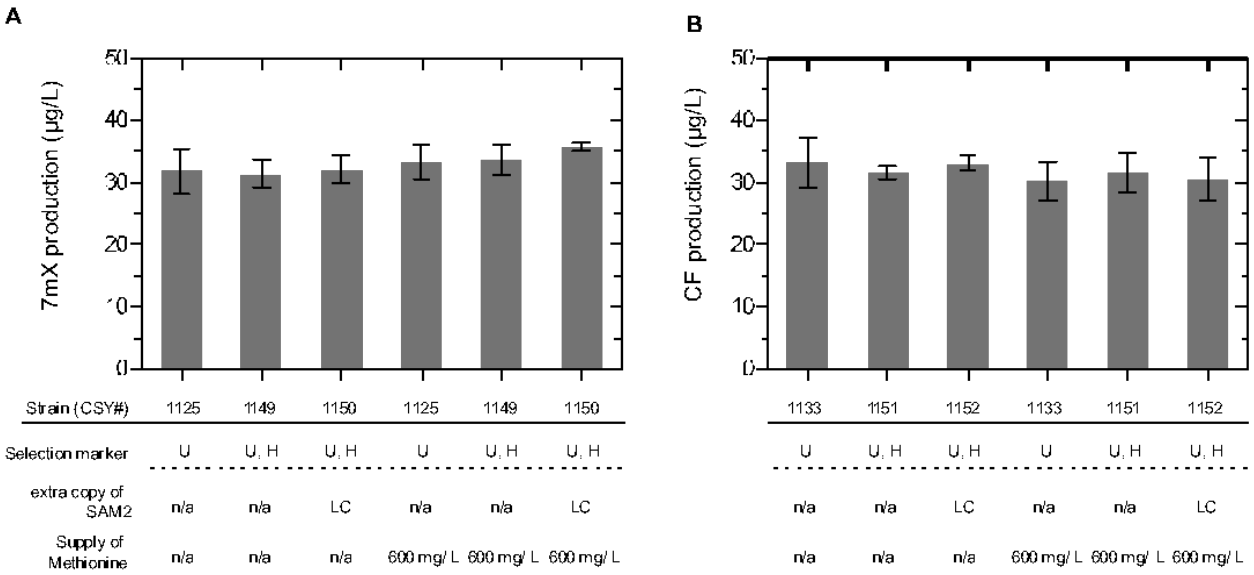

Fig. S8. Impact of overexpressing endogenous SAM2 with additional methionine. The production of (A) 7-methylxanthine, 7mX in engineered strain CSY1125 (B) caffeine, CF in engineered strain CSY1133. *SAM2* was overexpressed on a low-copy plasmid, and cells harboring an empty vector control were used for comparison in addition to the initial base strains. Fed methionine was supplied at 600 mg/L. Differences from *SAM2* overexpression and feeding high levels of L- methionine are not statistically significant.

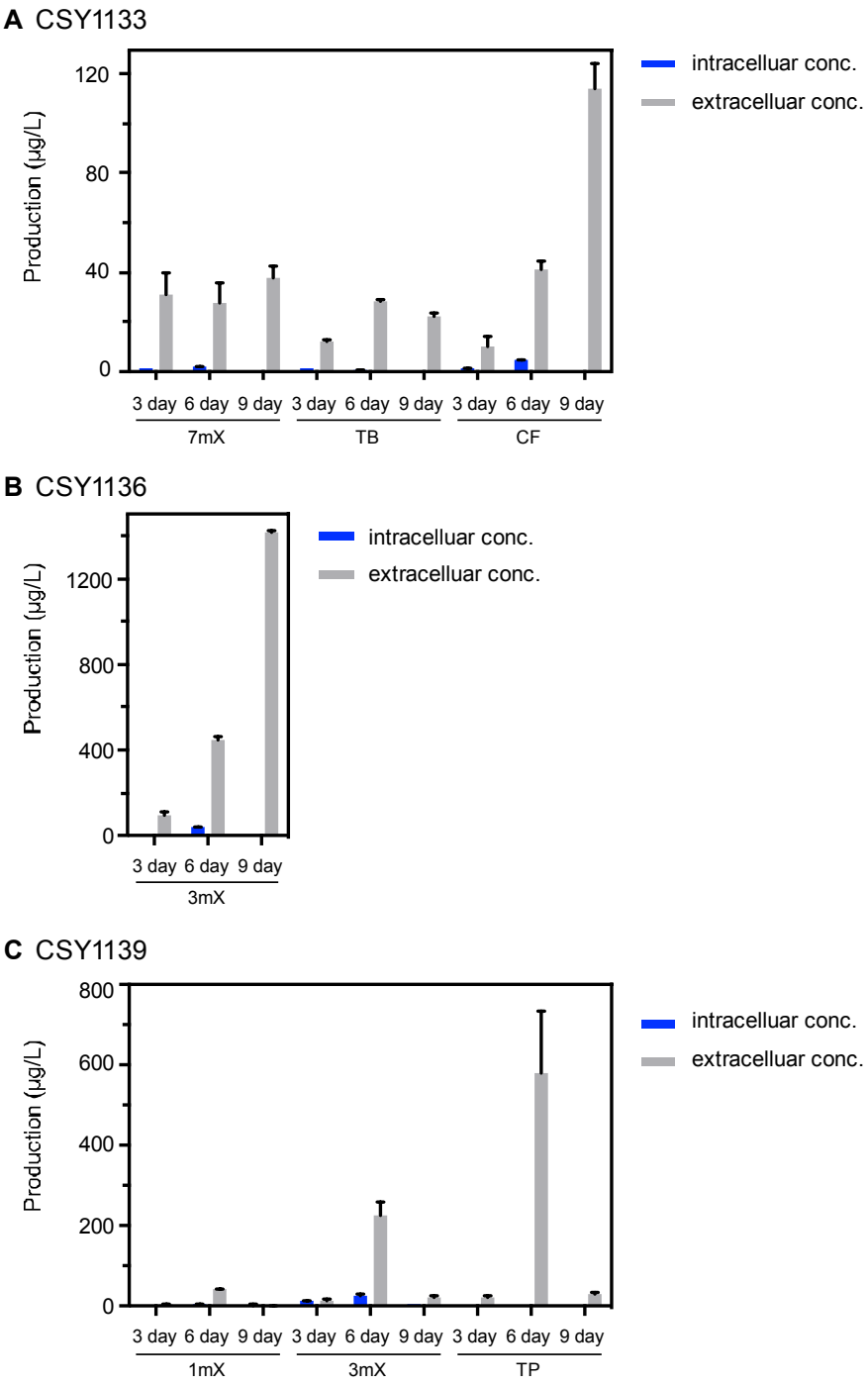

Figure S9. Comparison of intracellular and extracellular concentrations of methylxanthines. Titers of end-products in the cell pellets (intracellular, blue) or in the medium (extracellular, gray) are shown for CSY1133, 1136, and 1139 cultured after 3-9 days. Data are plotted as the mean values and error bars represent ± 1 s.d. of two biological replicates.

Table S1. Oligonucleotides used in this study.

Name	Sequence (5′ to 3′)
Genome integration of the yeast strain CSY1125	
4'OMT/lyp1_left_fwd	GGGCAGGTTTAGTAACATAATAACGTCCAATATGAACTCGTAAAAGCAAAGGTGGTTTCT
4'OMT/lyp1_left_rev	GGGCACCACACAAAAACGGACCTTAATACATTCAGACACTTCTGC
pCS3/4'OMT_fwd	TCTGAATGTATTAAGGTCCGTTTTTGTGTGGTGCCCTCCTCC
pCS3/6OMT_rev	TTGATAATGATAAACTCGAAGAGCTCCTAATGTCTGCCCCTATGTCTGCC
6OMT/pCS3_fwd	GACATAGGGGCAGACATTAGGAGCTCTTCGAGTTTATCATTATCAATACTCGC
6OMT/9OMT_rev	CGCTCGAAGGCTTTAATTTGTGATCTGCCGGTAGAGGTGTG
9OMT/6OMT_fwd	CCTCTACCGGCAGATCACAAATTAAAGCCTTCGAGCGTCCC
9OMT/lyp1_right_rev	TGTTCGCCAATGTTGTTTTGTTTCTCGTCCCATTATATGCATAGCTTCAAAATGTTTCTACTCC
4'OMT/lyp1_left_fwd	GGGCAGGTTTAGTAACATAATAACGTCCAATATGAACTCGTAAAAGCAAAGGTGGTTTCT
4'OMT/lyp1_left_rev	GGGCACCACACAAAAACGGACCTTAATACATTCAGACACTTCTGC
pCS3/4'OMT_fwd	TCTGAATGTATTAAGGTCCGTTTTTGTGTGGTGCCCTCCTCC
pCS3/6OMT_rev	TTGATAATGATAAACTCGAAGAGCTCCTAATGTCTGCCCCTATGTCTGCC
Knock-out yeast strains construction	
mmKO1_pCS3_fwd	TATATGGGCAGGTTTAGTAACATAATAACGTCCAATATTTTTGTGTGGTGCCCTCCTCC
mmKO2_pXMTI_fwd	GGAGCTCTTCGAGTTTATCATTATCAACAAATTAAAGCCTTCGAGCGTCC
mmKO3_pPA0065_rev	CTCTGTTCGCCAATGTTGTTTTGTTTCTCGTCCCATTTGATCTGCCGGTAGAGGTGTG
Colony PCR verification	
p28 lyp1 seq5'utr_fwd	AAAGTTTGCACCTCGTTCCC
p143 STE2 term_rev	GCTCATCAGATGCACCACATTC
p132 HsAID seq_rev	GGGACCTAGACTTCAGGTTGTCTAACTCC
p29 lyp1 seq3'ORF_rev	GACCAGTACCGATTGTACCACCTA

Table S2. Production of methylxanthines using: (A) CaMXMT1-only strain (CSY893 + pCS3526), (B) CaMXMT2-only strain (CSY893 + pCS3527), (C) CaDXMT1-only strain (CSY893 + pCS3529), and (D) CaXMT1-only strain (CSY893 + pCS3523) under different fed intermediate substrates.

(A) CaMXMT1-only strain

Fed substrate			Methylxanthine product titer (μg/L) and molar conversion efficiency (%)						
Type	Name	(100 μM-equivalent)	1mX	3mX	7mX	TP (1, 3)	PX (1, 7)	TB (3, 7)	CF (1, 3, 7)
No feeding (background)		-	ND	53.6 ± 0.9	ND	ND	ND	ND	ND
Un-methylated	XR	28.4 mg/L	ND	56 ± 7 (0.3 %)	ND	ND	ND	ND	ND
	XT	15.2 mg/L	ND	174 ± 19 (1 %)	ND	ND	ND	ND	ND
Mono-methylated	1mX	16.6 mg/L				ND	ND		ND
	3mX	16.6 mg/L				ND		ND	ND
	7mX	16.6 mg/L					ND	7350 ± 70 (40.8 %)	ND
Di-methylated	TP (1, 3)	18.0 mg/L							ND
	PX (1, 7)	18.0 mg/L							16 ± 2 (< 0.1 %)
	TB (3, 7)	18.0 mg/L							53 ± 2 (0.3 %)

(B) CaMXMT2-only strain

Fed substrate			Methylxanthine product titer (μg/L) and molar conversion efficiency (%)						
Type	Name	(100 μM-equivalent)	1mX	3mX	7mX	TP (1, 3)	PX (1, 7)	TB (3, 7)	CF (1, 3, 7)
No feeding (background)		-	ND	25 ± 2	ND	ND	ND	ND	ND
Un-methylated	XR	28.4 mg/L	ND	28 ± 3 (0.1 %)	ND	ND	ND	ND	ND
	XT	15.2 mg/L	ND	68 ± 8 (0.4 %)	ND	ND	ND	ND	ND
Mono-methylated	1mX	16.6 mg/L				ND	ND		ND
	3mX	16.6 mg/L				ND		ND	ND
	7mX	16.6 mg/L					ND	4938 ± 170 (27 %)	ND
Di-methylated	TP (1, 3)	18.0 mg/L							ND
	PX (1, 7)	18.0 mg/L							10 ± 2 (< 0.1 %)
	TB (3, 7)	18.0 mg/L							30 ± 5 (0.15 %)

(C) CaDXMT1-only strain

Fed substrate			Methylxanthine product titer (μg/L) and molar conversion efficiency (%)						
Type	Name	(100 μM-equivalent)	1mX	3mX	7mX	TP (1, 3)	PX (1, 7)	TB (3, 7)	CF (1, 3, 7)
No feeding (background)		-	ND	ND	ND	ND	ND	ND	ND
Un-methylated	XR	28.4 mg/L	ND	ND	ND	ND	ND	ND	ND
	XT	15.2 mg/L	ND	ND	ND	ND	ND	ND	ND
Mono-methylated	1mX	16.6 mg/L				ND	ND		ND
	3mX	16.6 mg/L				ND		ND	ND
	7mX	16.6 mg/L					ND	42 ± 9 (0.2 %)	ND
Di-methylated	TP (1, 3)	18.0 mg/L							10 ± 1 (< 0.1 %)
	PX (1, 7)	18.0 mg/L							595 ± 180 (3 %)
	TB (3, 7)	18.0 mg/L							454 ± 60 (2.4 %)

(D) CaXMT1-only strain

Fed substrate			Methylxanthine product titer (μg/L) and molar conversion efficiency (%)						
Type	Name	(100 μM-equivalent)	1mX	3mX	7mX	TP (1, 3)	PX (1, 7)	TB (3, 7)	CF (1, 3, 7)
No feeding (background)		-	ND	ND	6.1 ± 0.3	ND	ND	ND	ND
Un-methylated	XR	28.4 mg/L	ND	ND	86 ± 6 (0.5 %)	ND	ND	0.7 ± 0.3 (< 0.1 %)	ND
	XT	15.2 mg/L	ND	3 ± 0.9 (< 0.1 %)	14 ± 2 (< 0.1 %)	ND	ND	ND	ND
Mono-methylated	1mX	16.6 mg/L				ND	1.7 ± 0.9 (< 0.1 %)		ND
	3mX	16.6 mg/L				2.2 ± 0.3 (< 0.1 %)		ND	ND
	7mX	16.6 mg/L	not tested						

Note: The grayed-out regions are methylxanthine products that are not feasible in the reactions when feeding the indicated substrates, and the blue-meshed regions represent the fed substrates themselves. Product titer is presented in the upper part of a cell and the molar conversion efficiency is in the bottom part. Molar conversion efficiency is calculated by the molarity ratio between the product and the fed substrate. The high feeding concentration compared to the relatively low permeability of these molecules (Michener, 2012) across the cell membrane is one reason for the low molar conversions. Another likely reason is the high K_m values of all of the enzymes. Abbreviations: ND: not detectable.

Supplemental References

Brown, S., Clastre, M., Courdavault, V., and O'Connor, S.E. (2015). De novo production of the plant-derived alkaloid strictosidine in yeast. Proceedings of the National Academy of Sciences of the United States of America *112*, 3205-3210.

Choi, E.J., Bae, S.H., Park, J.B., Kwon, M.J., Jang, S.M., Zheng, Y.F., Lee, Y.S., Lee, S.J., and Bae, S.K. (2013). Simultaneous quantification of caffeine and its three primary metabolites in rat plasma by liquid chromatography-tandem mass spectrometry. Food chemistry *141*, 2735-2742.

Chu, J., Qian, J., Zhuang, Y., Zhang, S., and Li, Y. (2013). Progress in the research of S-adenosyl-L-methionine production. Applied microbiology and biotechnology *97*, 41-49.

Kunjapur, A.M., Hyun, J.C., and Prather, K.L. (2016). Deregulation of S-adenosylmethionine biosynthesis and regeneration improves methylation in the E. coli de novo vanillin biosynthesis pathway. Microbial cell factories *15*, 61.

Kuranda, K., Leberre, V., Sokol, S., Palamarczyk, G., and Francois, J. (2006). Investigating the caffeine effects in the yeast Saccharomyces cerevisiae brings new insights into the connection between TOR, PKC and Ras/cAMP signalling pathways. Molecular microbiology *61*, 1147-1166.

Ledesma-Amaro, R., Buey, R.M., and Revuelta, J.L. (2015). Increased production of inosine and guanosine by means of metabolic engineering of the purine pathway in Ashbya gossypii. Microbial cell factories *14*, 58.

Michener, J. (2012). Combining Rational and Evolutionary Approaches to Optimize Enzyme Activity in Saccharomyces cerevisiae. PhD Thesis Chapter 5.

Sandlie, I., Solberg, K., and Kleppe, K. (1980). The effect of caffeine on cell growth and metabolism of thymidine in Escherichia coli. Mutation research *73*, 29-41.

Schlenk, F., and Depalma, R.E. (1957). The formation of S-adenosylmethionine in yeast. The Journal of biological chemistry *229*, 1037-1050.